

**How to Cite:**

Sahu, T., Jain, A. P., & Jain, P. (2022). Preparation, characterization and pharmacological evaluation of topical hyalurosomes nanogel formulation of *Calotropis gigantea* for the treatment of Vitiligo. *International Journal of Health Sciences*, 6(S10), 807–829. Retrieved from <https://sciencescholar.us/journal/index.php/ijhs/article/view/13661>

# **Preparation, characterization and pharmacological evaluation of topical hyalurosomes nanogel formulation of *Calotropis gigantea* for the treatment of Vitiligo**

**Tilotma Sahu**

Faculty of Pharmacy, Sarvepalli Radhakrishnan University, Bhopal

**Alok Pal Jain**

Faculty of Pharmacy, Sarvepalli Radhakrishnan University, Bhopal

**Pratyush Jain\***

Associate Professor, Faculty of Pharmacy, SRK University Bhopal

\*Corresponding author

**Abstract**--Objective: The objective of the paper is to preparation, characterization and pharmacological evaluation of topical hyalurosomes nanogel formulation of *Calotropis Gigantea* for the treatment of Vitiligo. Material and methods: Fresh milky white latex of *Calotropis Gigantea* was collected by cutting the stem twigs and identified by the HPLC method for phytoconstituents. Hyalurosomes as nanogel formulation was prepared by the solvent evaporation-based ethanol injection method. The nanogel was characterized for the particle size, Zeta-potential, poly dispersity index, transmission electron microscope, viscosity, entrapment efficiency and *In-vitro* release. The Carbopol based gel formulation was prepared and compare with the nanogel formulation. Fluorescent Rhodamine loaded hyalurosomes nanogel formulation (CGHGF) was prepared and utilized for cell uptake studies. The nanogel for anti-vitiligo activity was evaluated by cell uptake studies, cell viability assay, melanin content assay, tyrosinase activity assay and Fontana-Masson silver staining on B16F10 cell line. Result: The compounds present in the latex of *Calotropis Gigantea* includes lupeol, beta-amyrin, alpha-calotropeol, and beta-calotropeol, and tetracyclic compounds, including uscharin and 20-epi-uscharin, were characterized using HPLC method. The prepared hyalurosomes nanogel having the particle size  $154.90 \pm 1.7$ , Poly-dispersity index was found to be 0.28 with zeta

potential -17.00. The entrapment efficiency was found to be 84.56%. Quantitative dye uptake into cells  $60.60 \pm 3.23\%$  uptake with Fluorescent Rhodamine-CGHGF as compared to the Fluorescent-rhodamine solution showed about  $32.01 \pm 4.85\%$  uptake. Cell viability assay stated that CGHGF showed  $68.71 \pm 2.76\%$  cytotoxicity, as compared to CG-Carbopol Gel ( $52.10 \pm 9.63\%$ ) at  $50 \mu\text{M}$  concentration. The CG-Carbopol gel showed  $56.11 \pm 11.55\%$  cytotoxicity and CGHGF has shown the  $82.95 \pm 11.61\%$  cytotoxicity at  $50 \mu\text{M}$  concentration. Discussion: The *Petroleum ether* latex of *Calotropis Gigantea* loaded-hyalurosomes (CGHGF) and CG-Carbopol Gel were successfully prepared with particle size of  $<150 \text{ nm}$  and high entrapment efficiency. Unique deformable nature of hyalurosomes and CG-Carbopol gel also assists in skin penetration enhancement of latex containing active constituents. Higher encapsulation of loaded drugs reduces the drug dose and sustained release of *Petroleum latex* of *Calotropis Gigantea* loaded-hyalurosomes (CGHGF) and CG-Carbopol Gel avoids frequent drug administration. Cell uptake studies confirmed higher penetration of encapsulated moiety through prepared CGHGF.

**Keywords**--hyalurosomes, *calotropis gigantea*, HPLC, B16F10 cell line, cell uptake.

## Introduction

Vitiligo (leukoderma) is recognized as a common skin pigmentation disorder stemming from progressive selective destruction of epidermal melanocytes operating as pigmentation cells. Vitiligo is an acquired idiopathic, dermatological disorder characterized by well circumscribed milky white macules devoid of identifiable melanocytes.<sup>[1]</sup> These asymptomatic white macules can be psychologically extremely damaging, even leading to attempted suicide in some cases. It affects approximately 1% of the world's population and approximately 3-4% of the Indian population. The most common sites of involvement are the face (24.5%), neck (18.8%), and scalp (11.2%). The vitiligo results in obvious flat white lesions in normally pigmented skin, which commonly appear on face, arms, hands, feet, and lips. Patches may be progressive and arise at any age.<sup>[2]</sup>

Exposure to environmental stressors, such as ultraviolet (UV) radiation and numerous chemicals, usually affects epidermal cells, including melanocytes, which leads to an increase in the production of reactive oxygen species (ROS). Vitiligo patients have intrinsic defects in their melanocytes, which diminishes the cell ability to respond well to cellular stressors. Therefore, increased concentrations of epidermal  $\text{H}_2\text{O}_2$  and decreased concentrations of catalase, which protect cells from oxidative destruction, have been found. The rationale of vitiligo treatment is to control immunoreactions by suppressing oxidative stress and restoring the normal skin colour in the affected area through formation of healthy melanocytes instead of damaged ones.<sup>[3]</sup>

To date, no curative therapy is available for vitiligo. In many years, vitiligo therapy has depended on systemic therapy, topical agents, phototherapy, and surgical techniques, which all aim to reduce disease progression and stimulate skin repigmentation. The chronic nature of the disease and long-term therapy with the lack of uniform treatment are very demoralizing for vitiligo patients. The natural treatment approaches for management of vitiligo have been concerned such as using hypericin, khellin, and berberine are considered as effective therapeutic tools for the treatment of vitiligo.<sup>[4]</sup> Recently, Nano-dermatology science applies nanotechnology approaches in the field of dermatology and have involved sunscreens and maintenance of skin health as well as providing a tool for the diagnosis and management of skin disease and transport bioactive compounds at effective concentrations over a predetermined period. Such tactic has been directed toward enhancement of the activity problems of many biologically active compounds via improving drug solubility, skin deposition, skin permeability as well as minimize toxicity.<sup>[5]</sup>

Sodium hyaluronate (hyaluronan) is the sodium salt form of hyaluronic acid that present in human organs as part of numerous connective tissues, lungs, synovial fluid, and muscle tissues. It is considered to be a dual functioning component that has been used as a viscosity enhancer in skin care products and to improve dehydrated skin by replenishing the hyaluronic acid content.<sup>[6]</sup> Hyalurosomes are a modified nanovesicles that possess the intrinsic characteristics of phospholipid nanovesicles potentiated with hyaluronan penetration enhancer and gelling capabilities. Consequently, hyalurosomes combine the privileges of both elastic features of deformable liposomes and the stability of gel-core vesicles. Hyalurosomes would provide many benefits in local skin delivery owing to hyaluronan such as; longer residence time at the application site, penetration enhancing ability, hence facilitating skin permeation and drug deposition.<sup>[7]</sup>

Therefore, loading of drug in hyalurosomes are expected to yield an outstanding outcome by enhancing the low skin permeability of *Calotropis Gigantea* latex providing promising antioxidant and anti-inflammatory effects. Consequently, the current study is the first work to represent topical *Calotropis Gigantea* latex-hyalurosomes nanogel as a targeted nano-therapy to enhance the skin permeability and deposition of drug for treatment of vitiligo.<sup>[8]</sup> The natural product obtained from the plant sources pay attention towards the management and treatment strategies for Vitiligo patients. The main approaches of the research work are to focus on the herbal based nano-formulation (hyalurosomes) Petroleum latex of *Calotropis Gigantea* to enhance therapeutic activity and skin permeation and evaluated them for anti-vitiligo activity. The topical route may improve the bioavailability and efficacy of the treatment of Vitiligo as well as minimize toxicity.

## Materials and Methods

Lipoid® S100 (1- $\alpha$ -phosphatidylcholine) was obtained as gift sample from Lipoid AG (Ludwigshafen, Germany). Sodium hyaluronate (hyaluronan) was Purchased from Euromedex, (France). The Petroleum ether Latex of *Calotropis Gigantea* were used as drug for encapsulation in polymeric nanocarrier. Hydroquinone and carbopol-940 were purchased from Sigma-Aldrich, New Delhi. Sodium deoxy

cholate (SDC), bovine serum albumin, acridine orange (AO), nuclear fast red and cellulose dialysis tubing with 12000 Da molecular weight cut off was purchased from Hi-Media, Mumbai, India. Chloroform, methanol and acetonitrile were obtained from Merck Pvt Ltd. Mumbai, India. All other chemicals and reagents used were of analytical grade.

### **Extraction and Identification of *Calotropis Gigantea* plant**

Fresh milky white latex of *Calotropis Gigantea* was collected by cutting the stem twigs and identified by its active constituent by the HPLC method. Moist Lax was dried under open air during the day.<sup>[9]</sup> The dried Lax was divided in two parts; the first sample was evaluated for its solubility in various solvents such as hexane, ethyl ether, chloroform, ethyl acetate, butanol, methanol, acetone, acetonitrile, and water. The maximum solubility was observed in Petroleum ether and methanol. The latex derived compounds were identified using HPLC with a chromatography pump Shimadzu LC-6AD (Kyoto, Japan), C18 column (enable C18G 250×4.6 mm), and HPLC-grade methanol and water as the mobile phase.<sup>[10]</sup> The solid powder (dried extracts) was obtained by evaporation of the content in ELISA rotary evaporator were stored in air tight containers at 4°C till further use.<sup>[11]</sup>

### **Preparation and characterization of Topical hyalurosomes nanogel (CGHGF)**

A solvent evaporation-based ethanol injection method was used for the preparation of hyalurosomes nanogel with some modification.<sup>[12]</sup> Briefly L- $\alpha$ -phosphatidylcholine (5% w/v) and sodium deoxy cholate (SDC; 3.25%w/w) was dissolved in 2 ml of absolute ethanol. Then, the resulting ethanolic solution was injected dropwise through a 23-G syringe into a 10-ml hydrating medium solution containing hyaluronan (2.5%w/v) and petroleum ether latex of *Calotropis Gigantea* as drug (0.25%w/w, 5 mg) in water: ethanol (80:20) under constant magnetic stirring at 1500 rpm and room temperature for 90 min.<sup>[13]</sup>

Hyaluronan was used as a self-gelling agent at a concentration of 2.5%(w/v). Furthermore, the prepared dispersion was subjected to homogenization at 10,000 rpm for 10 min followed by sonication for 10 min and finally the dispersion was hermetically sealed and kept overnight in a refrigerator (4°C) for stabilization before further characterization and optimized by particle size and polydispersity index (PDI).<sup>[11-18]</sup> The placebo- hyalurosomes (CGPHGF) was prepared by same procedure without using the latex (drug). Fluorescent Rhodamine loaded CGHGF-8 (Rhodamine-CGHGF) were also prepared using optimized molar ratio for cell uptake studies. For preparation of dye loaded CGHGF, dye was mixed with lipid mixture and other steps were followed similar to Hyalurosomes.

### **Preparation of conventional Carbopol gel formulation loaded with Petroleum ether latex of *Calotropis Gigantea* (CG-Carbopol Gel)**

A petroleum ether latex of *Calotropis Gigantea*-loaded conventional Carbopol hydrogel was prepared as a control gel for comparison with hyalurosomes.<sup>[19]</sup> Gel was prepared by dispersing 5 mg of petroleum ether latex of *Calotropis Gigantea* (0.25% w/v) in 20 ml of distilled water. One gram of carbopol-940 was added

portion-wise under magnetic stirring until a gel was obtained at room temperature. [20]

### **Characterization of the Hyalurosomes formulation Determination of Particle size, zeta-potential, and poly-dispersity index**

The hyalurosomes nanogel was characterized for the particle size, zeta-potential, and poly dispersity index (PDI) were determined for both placebo hyalurosomes (CGPHGF) and Petroleum ether latex of *Calotropis Gigantea* loaded hyalurosomes (CGHGF) by means of dynamic light scattering (DLS) technique using Zeta sizer Nano ZS. (Malvern, Instruments Ltd., Malvern, UK). Prior measurements, all of the prepared formulations were appropriately diluted with freshly filtered distilled water and then sonicated for 5 min. Each sample was detected three times over 10 min. [21] All measurements were examined at 25°C in triplicates and results were demonstrated as mean value ± SD.

### **Transmission electron microscopy (TEM)**

Morphological examination was observed via Transmission electron microscope (TEM) (JEM-100S microscope; JOEL Ltd, Tokyo, Japan) to visualize the morphology of both CGPHGF) and CGHGF vesicles in aqueous solution. samples were subjected to dilution with distilled water (1:20) and exposed to sonication for 20 s. A thin film was attained by adding a drop of sample into a carbon-coated copper grid and then stained with an aqueous solution of uranyl acetate (1% w/v). Excess staining solution was removed with the aid of a filter paper and followed by air-drying. Afterwards, the stained air-dried film was examined under TEM and photographed. [22]

### **Rheological studies**

The viscosity of the CGPHGF, CGHGF and CG-Carbopol Gel was examined using a cone and plate Brookfield viscometer (USA) with a spindle 40). Sample was subjected to various speed ranging from (8-200 rpm) and the measurements were performed at room temperature (25±2°C). [23]

### **Determination of entrapment efficiency (EE%)**

Percentage entrapment efficiency (%EE) was determined by ultrafiltration using Centrisarts® (MWCO 100000, Sartorius, Bohemia, NY, USA). About 2.5 ml of the prepared CGHGF formulation were added into the outer chamber and sample recovery chamber was positioned on top of the sample and centrifuged at 3000 rpm for 20 min at room temperature. The amount of drug in the filtrate was measured UV-spectrophotometrically at 530 nm. [24]

The entrapment efficiency percent was calculated by the following Eq. (1):

$$EE\% = [(A2 - A1)/A2] \times 100 \dots \dots \dots (1)$$

Where A1 is the amount of free Petroleum ether latex of *Calotropis Gigantea* content and A2 is the total amount of Petroleum ether latex of *Calotropis Gigantea* content in the formulation.

### ***In-vitro* release behaviour**

Dialysis bags (MWCO 12,000-14,000) were used to determine in-vitro release profiles. The bags were previously soaked in distilled water for 24h and tightly sealed. 1 ml samples of Petroleum ether latex of *Calotropis Gigantea* solution, CG-Carbopol Gel and CGHGF, all containing an amount of drug equivalent to 5 mg of powder extract of Petroleum ether latex of *Calotropis Gigantea* were then placed into stoppered glass vials containing 10 ml of acetate buffer (pH 5) as a dissolution medium. The vials were stored at  $32\pm 0.5^\circ\text{C}$  with 100 rpm shaking in a thermostatic shaking water bath throughout the experiment.<sup>[25]</sup> A 2-ml sample volume was withdrawn at fixed time intervals (0.25, 0.5, 0.75, 1, 2, 3, 4, 5, 24 h) and replaced with an equal volume of fresh buffer to maintain the sink conditions.<sup>[26]</sup> The average cumulative percentage of drug released at different time intervals was plotted to determine different drug-release profiles. Drug concentration was calculated spectrophotometrically by measuring UV absorbance at a wavelength of 530 nm against a corresponding appropriate blank buffer solution.<sup>[27]</sup> Each experiment was examined as triplicates. Data were expressed as the mean $\pm$ SD.

### **Pharmacological Evaluation**

#### **Evaluation studies on B16F10 cell line**

Melanocyte cells (B16F10) used in the study were procured from the National Center for Cell Science, Pune and were cultured in Dulbecco's Modified Eagle's Medium (DMEM) containing 10% heat inactivated fetal bovine serum, 1.5g/L  $\text{NaHCO}_3$ , 2mM L-glutamine, 10,000 units penicillin, 10 $\mu\text{g}/\text{mL}$  streptomycin, and 25 $\mu\text{g}/\text{mL}$  amphotericin B, incubated at  $37^\circ\text{C}$  with 5%  $\text{CO}_2$  in a humidified atmosphere.<sup>[28]</sup>

#### **Cell uptake studies**

For cell expansion and experiments with isolated cells, the B16F10 cells were detached with 1X Trypsin-EDTA solution. Cells were seeded in a 12 well plate at a density of  $1\times 10^5$  cells/well in the respective media and allowed to adhere for 24hrs. Then the cells were incubated with Rhodamine solution and Rhodamine-CGHGF at different concentrations (1, 5 and 10  $\mu\text{M}$ ) for 3hrs. Further, the media was removed and cells were washed twice with phosphate buffered saline (PBS). Nuclear staining was performed using acridine orange (AO) stain (1 mg/ml) and the stain was removed immediately after 30 sec.<sup>[29]</sup> Washing step was repeated and then phase contrast followed by fluorescent images was taken using fluorescent microscope (Nikon Eclipse Microscope, Japan). Quantitative dye uptake into cells was measured with fluorescent rhodamine solution and fluorescent rhodamine-CGHGF at 10 $\mu\text{M}$  dye concentration. To quantify the uptake of dye, media was removed and cells were washed twice with PBS. Cell lysis was carried out using Triton X-100. The cell uptake of dye was quantified by

measuring the fluorescence in the cell lysate.<sup>[30]</sup> Results were expressed as % cellular uptake.

### **Cell viability assay**

Cells were seeded in 96-well plates at a density of  $1 \times 10^4$  cells per well and incubated for 24h. Initially cells were treated with *Petroleum latex of Calotropis Gigantea* as drug (0.25%w/w, 5 mg) solutions at 10 to 250 $\mu$ M equivalent drug concentrations to obtain 50% cell growth inhibitory concentration (IC<sub>50</sub>) for the respective drugs. After 24h incubation period, fresh DMEM containing 500 $\mu$ g/ml of 3-(4,5-Dimethylthiazol-2-yl)-2,5-diphenyltetrazolium bromide (MTT) was added to replace the formulations and incubated for 3h.<sup>[31]</sup> MTT solution was aspirated and dimethyl sulphoxide (DMSO) was added to dissolve the formazan crystals. Absorbance was measured at 570 nm using microplate reader (Spectramax, Molecular Devices LLC, USA).<sup>[32]</sup> Untreated cells were taken as control with 100% viability and cells without addition of MTT were used as blank. Based on the results from above assay, cells were treated with test formulations petroleum latex of *Calotropis Gigantea* loaded hyalurosomes (CGHGF) and CG-Carbopol gel at 1 to 50 $\mu$ M concentration range. After 24h exposure of cells to different formulations determined the effect of formulations on cell viability.<sup>[33]</sup>

### **Melanin content assay**

B16F10 cells were seeded in two 12 well plates at a density of  $1 \times 10^5$  cells/well and incubated for 24 hrs. For evaluating the effect of first treatment (cells were treated once), the media was replaced by test formulations equivalent to 5  $\mu$ M concentration of each drug followed by UV exposure for groups. After 48 hrs. of exposure to formulations, cells were processed for further steps. For another 12-well plate, second treatment was also given (cells were treated twice) and similar procedure was followed as per first treatment. Media from the first treatment was replaced by fresh media containing formulations at 48 hrs. (followed by UV exposure for PSR groups) and incubated for additional 48 hrs. After 48 hrs. exposure (for first treatment) and 96 h exposure (for second treatment), cells were washed twice with PBS and lysed by incubation in lysis buffer (PBS with 1% Triton X-100) at 4 °C for 20 min.<sup>[34]</sup>

The lysates from both the plates were centrifuged separately at 14000 rpm for 15 min to collect the pellet. Supernatants were processed for tyrosinase activity determination whereas the cell pellet is dissolved using 1N sodium hydroxide (NaOH) containing 10% DMSO for 1h at 80°C to solubilize the melanin. The protein estimation was performed using Bradford's assay and bovine serum albumin was taken as a standard. Aliquots containing same amount of protein were taken and volume was made up to 100 $\mu$ L with NaOH solution. Absorbance was measured for samples at 366 nm and melanin content was calculated from a standard curve using synthetic melanin.<sup>[35]</sup>

### **Tyrosinase activity assay**

Cell supernatant obtained from the above procedure was analysed using Bradford's assay for its protein content. Samples containing same amount of

protein were taken, volume was made up to 100 $\mu$ L with lysis buffer and then 0.1% L-DOPA solution prepared in PBS (100  $\mu$ L) was added to it. The plate was incubated at 37°C for 1h and the dopachrome was monitored by measuring the absorbance at 475 nm. [36]

### **Cell free tyrosinase assay**

A cell-free assay system was used to test direct effects of CGHGF on tyrosinase activity. About 130  $\mu$ l of sample dilutions prepared from test formulations at 1 to 50  $\mu$ M concentration range were mixed with 20  $\mu$ l of mushroom tyrosinase (1000 units) and 100  $\mu$ l of L-DOPA solution (2 mg/ml). The assay mixtures were incubated at 37 °C for 20 min and absorbance of dopachrome was measured at 475 nm in a microplate reader. The mushroom tyrosinase activity was calculated and compared with control.[37]

### **Fontana-Masson silver staining**

Cells were seeded in a 12 well plate at a density of  $5 \times 10^4$  cells/well in the respective media and incubated for 24 h. Then the media was replaced by CGHFG formulations (5  $\mu$ M equivalent drug concentration), followed by UV exposure and incubated for 24 h. Later, the cells were washed and fixed in 4% v/v formalin followed by staining with 2.5% w/v ammonical silver nitrate (temperature maintained at 56°C). The plate was incubated for 1hrs. and then washed with distilled water. Then 5% w/v sodium thiosulfate solution was added, incubated for 5 min and washed with distilled water. Later, the cells were stained with nuclear faster red solution for 5 min and washed again. Finally, after dehydration with ethanol the wells were washed with xylene twice. Then the plate was observed under phase contrast microscope for visualization of melanin pigment in wells. [38]

## **Results and Discussion**

### **Identification of phytoconstituents by HPLC methods**

The compounds present in the Latex of *Calotropis Gigantea* (family: Apocynaceae) such as lupeol, beta-amyrin, alpha-calotropeol, and beta-calotropeol, and tetracyclic compounds, including uscharin and 20-epi-uscharin, were characterized using HPLC. The compounds identified from *Calotropis Gigantea* Lax were compared with previous reports by Periyakaruppan PK et al., 2017.[39] The usharin, calotoxin, and calactin were identified in the methanol portion using methanol and water in the mobile phase. Lupeol was detected in the Petroleum ether and beta-amyrin was present in the water fraction. The derived of Lax compounds in a column, using water as a solvent, revealed four major peaks and three minor peaks (Figure 1a).

The major peaks were at retention times of 9.56, 11.01, 13.88, and 14.84 min and the minor peaks were at 8.64, 9.86, and 10.01 min. These peaks were previously reported at retention times of 9.56 min for the lupeol compound, beta-amyrin at 10.01 min, and uscharin at 8.640 min. In the derived of Lax using Petroleum ether and methanol, the peaks were observed at 9.644 min (lupeol) and

at retention times of 8.99 min (uscharin), 11.620 min (calotropin), and 13.580 min (calactin) (Fig. 5.1B and 5.1C). HPLC was used to further identify the Lax compounds using chloroform with ethyl acetate (80:20 and 50:50) as solvents as shown (Fig. 5.1D and 5.1E). The  $\text{CHCl}_3$ /ethanol (80:20) peaks at 14.359 min were correlated to calactin and the  $\text{CHCl}_3$ /ethanol (50:50 v/v) peak at 15.157 min.

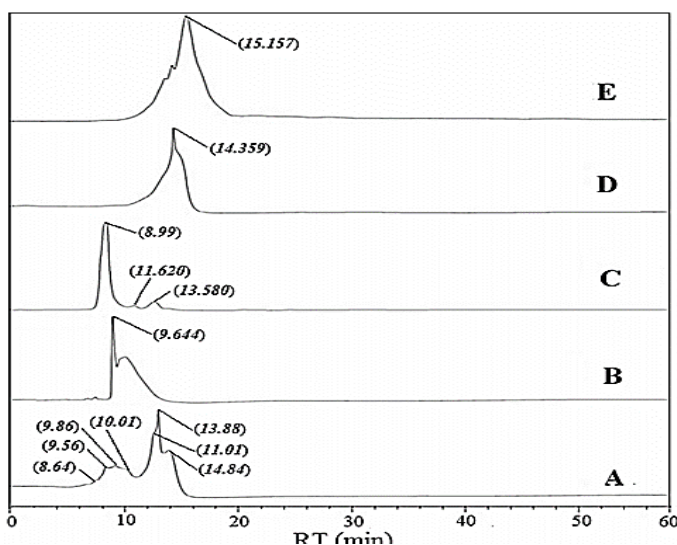


Figure 1. HPLC-chromatogram analysis of the water latex extraction *Calotropis Gigantea* and derived compounds (A) pure latex, (B) pet-ether latex, (C) methanol latex, (D)  $\text{CHCl}_3$ /ethanol (80:20), and (E)  $\text{CHCl}_3$ /ethanol (50:50)

### FTIR analysis

The functionality of the Latex compounds was characterized by FTIR spectroscopy (Fig. 5.2). The FTIR spectrum of pure Latex (A), Petroleum ether portion of latex (B), and methanol portion of latex (C) was determined. A broad peak at  $3253\text{ cm}^{-1}$  was noted, this is response to the OH stretching frequencies of uscharin, calotropin, lubeol, and b-amyrin. High intense broad peaks were appeared at  $1628\text{ cm}^{-1}$  of di-ketonic bonds. The peaks at  $1065\text{ cm}^{-1}$  corresponded to the C-N stretching bonds of aliphatic amines. The Petroleum ether soluble lax was identified to determine the characteristics of the compounds based on FTIR spectrum (Fig. 5.2B) and compared with FTIR spectrum of pure latex (Fig. 5.2A). The OH stretching frequency peak was not present, confirming that polar compounds were not present in the Petroleum ether portion. Other characteristic peaks indicated a COOH stretching vibration at  $2975\text{ cm}^{-1}$  and bending vibration at  $1320\text{ cm}^{-1}$ . Polar solvent soluble compounds showed a broad peak at  $3375\text{ cm}^{-1}$  because of the OH group of the polar molecules (Fig. 5.2C).

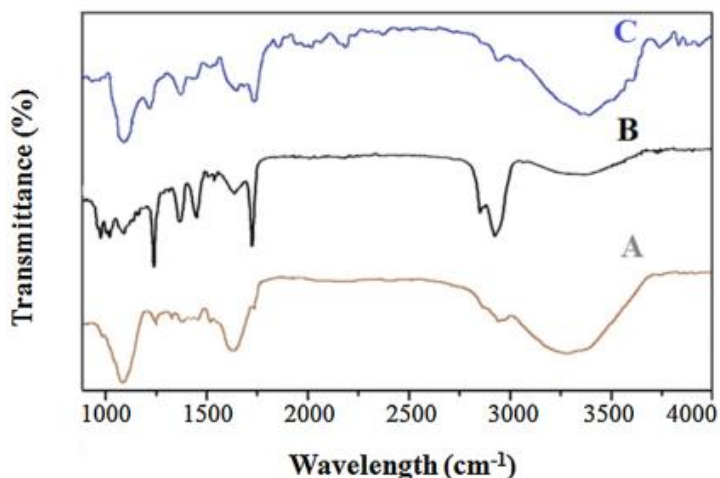


Figure 5.2. FTIR spectra of samples: (A) pure latex; (B) Petroleum ether latex; (C) methanol latex

### Fluorescent studies

The Fluorescent studies of latex of *Calotropis Gigantea* by UV spectrophotometry stated that at visible-light the latex has shown the Yellowish white, at Short UV light (252 nm) Light yellow colour is shown and at Long UV light (366 nm) Alice blue colour is seen. The Petroleum ether latex at Visible light has shown the light cream, at Short UV light (252 nm) Yellowish Green colour is shown and at Long UV light (366 nm) cream colour is seen. The methanol latex at Visible light has shown the light yellow, at Short UV light (252 nm) Yellowish Green colour is shown and at Long UV light (366 nm) brown colour is seen. The *Petroleum ether latex of Calotropis Gigantea* contain the lupeol, beta-amyrin (Water fraction of latex), alpha-calotropeol, and beta-calotropeol used as drug for the Topical Nano delivery of therapeutics. The Petroleum ether contains lupeol, beta-amyrin, alpha-calotropeol, and beta-calotropeol, so Petroleum ether latex of *Calotropis Gigantea* is used as drug for treatment of vitiligo by topical nanocarrier drug delivery system.

### Development and optimization of Hyalurosomes formulation

The rationale for selection of hyaluronan as a key ingredient in the hyalurosomes formulation was that it is a natural non-irritant, allows deep skin penetration, and is self-gelling. Moreover, because there is a direct relationship between the viscosity of hyaluronan and its concentration, increasing its concentration from 0.2% to 3% could successfully convert liquified-HS into more viscous hyalurosomes gel formulation. Consequently, novel Petroleum ether latex of *Calotropis Gigantea* loaded hyalurosomes (CGHGF) was prepared for use as a topical formulation with more effective direct skin contact.

A preliminary study regarding the preparation method of hyalurosomes either by the solvent-evaporation based ethanol injection method was utilized. Formulation factors, such as stirring speed, homogenization time, and sonication time, were

optimized to yield small vesicles with good homogeneity, as shown in (Table 1). The results showed that by increasing the stirring speed from 900 to 1500 rpm, the vesicle size and PDI decreased by 3.5-fold, and there was a 1.5-fold improvement in homogeneity, so the stirring speed was set to 1500 rpm. On the other hand, increasing the homogenization time from 5-10 min yielded a further increase in PS by about 1.8-fold and in PDI by 1.3-fold.

Table 1  
Optimization factor for preparation of Hyalurosomes by ethanol injection method using different magnetic stirrer speed, homogenization and sonication time

S. No.	Formula Code	Stirrer Speed	Homogenization time (min)	Sonication time (min)	PS±SD	PDI±SD	ZP±SD
1.	CGHGF-1	900	00	00	2338.50±3.5	1.00±0.01	-17.50±0.17
2.	CGHGF-2	900	10	05	315.50±5.0	0.58±0.05	-18.20±0.19
3.	CGHGF-3	900	20	10	288.45±6.0	0.73±0.07	-19.50±0.11
4.	CGHGF-4	1200	00	00	645.65±3.0	0.65±0.02	-18.25±0.21
5.	CGHGF-5	1200	10	05	521.40±4.5	0.42±0.04	-18.75±0.19
6.	CGHGF-6	1200	20	10	256.50±2.5	0.35±0.02	-18.95±0.16
7.	CGHGF-7	1500	00	00	550.60±3.0	0.38±0.03	-18.40±0.15
8.	CGHGF-8	1500	10	05	115.90±1.9	0.28±0.01	-21.00±0.12
9.	CGHGF-9	1500	20	10	245.50±2.8	0.55±0.03	-18.58±0.13

The homogenization time was optimized for 10 min. Finally, the effect of sonication time demonstrated that, by applying an additional 5 min of sonication, the PS decreased by about 2.1-fold and the PDI by 2.1-fold. In conclusion, the optimized CGHGF-8 formulation was selected for further investigations with optimization factors set to a stirring speed of 1500 rpm, homogenization period of 10 min, and an increase in sonication time by 05 min.

### Physicochemical properties

The results of measuring the quality attributes of CGPHGF, and CGHGF were depicted in Table 2. A higher concentration of the polyanion hyaluronan resulted in a higher surface negative charge (1.3-fold) than that for CGPHGF. Consequently, CGHGF demonstrated improved homogeneity (PDI=0.28±0.01) with a smaller PS due to electrostatic repulsive forces. Moreover, the gel structure caused immobilization of the particles within the gel matrix and hence, more stability than in the liquid formulation.

Table 2  
Physicochemical properties of Hyalurosomes

S. No.	Formula code	Vesicle	PDI	Zeta Potential	Entrapment Efficiency
1.	Placebo hyalurosomes (CGPHGF)	115.90±1.9	0.28±0.01	-21.00±0.12	NA
2.	Petroleum ether latex of <i>Calotropis Gigantea</i> loaded-hyalurosomes (CGHGF)	154.90±1.7	0.28±0.02	-17.00±0.14	84.56±2.65

The Petroleum ether latex of *Calotropis Gigantea* loading as drug affected the hyalurosomes characteristics by increasing the particle size more than that in the placebo hyalurosomes. This effect may be because of the intercalation of positive charge of Petroleum ether latex of *Calotropis Gigantea* in the lipid bilayer with negatively charged phospholipids and hyaluronan. This explanation is further supported by the decrease in the ZP of hyalurosomes to that in the placebo hyalurosomes (due to the positive nature of latex) with no significant effect on the formulation homogeneity (PDI=0.28±0.05). Finally, Petroleum ether latex of *Calotropis Gigantea* loaded-hyalurosomes (CGHGF) yielded a high entrapment efficiency percentage (EE%) of 84.56±2.65%.

### Stability study

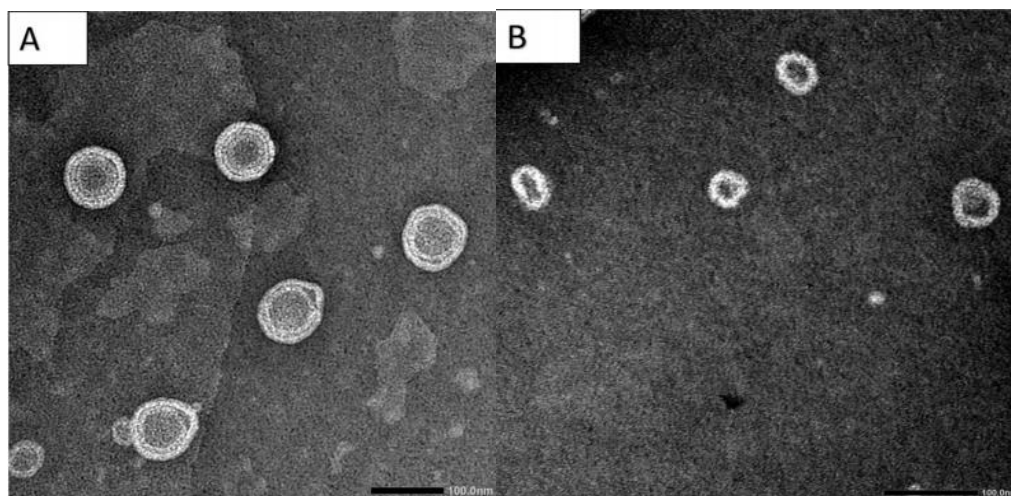
Upon storage for 6 months, the optimized preparation did not show any signs of instability at 4°C (Table 3). This may be ascribed to the hyaluronan interaction with choline groups on the phospholipid bilayer forming a structured self-gelling vesicle-polymer system. The intercalated high-viscosity matrix conferred superior stability to the hyalurosomes, which maintained the stability of their physicochemical features during storage (6 months at 4±1°C).

Table 3  
Stability study for CGPHGF and CGHGF stored in refrigerator at 4±1°C within 6 months

Code	Initial				3 months				6 months			
	Size (nm)	PDI	Zeta (mV)	EE (%)	Size (nm)	PDI	Zeta (mV)	EE (%)	Size (nm)	PDI	Zeta (mV)	EE (%)
CGPHGF	115.9 ±1.9	0.28 ± 0.01	-21.00 ± 0.12	NA	125.90 ±1.3	0.32 ± 0.05	- 19.00 ± 0.12	NA	133.9 ±1.2	0.48 ± 0.01	- 17.00 ± 0.12	NA
CGHGF	154.9 ±1.7	0.32 ± 0.01	-17.00 ± 0.14	84.56 ±2.65	156.90 ±2.1	0.34 ± 0.02	- 15.00 ± 0.14	80.56 ±1.52	158.5 ±1.3	0.48 ± 0.01	- 14.00 ± 0.14	78.50 ±2.50

### Morphological characterization by TEM

Morphological examination by TEM for CGPHGF and CGHGF. Micrographs illustrated the presence of well-dispersed shell-core vesicles clearly identified with a bilayer shell structure (Figure 3a). In addition, both hyalurosomes formulations appeared almost spherical with no aggregation, indicating the advantage of the gel form. On the other hand, a slightly dense shell layer appeared in Petroleum ether latex of *Calotropis Gigantea* hyalurosomes micrograph (Figure 3b), which may indicate the presence of Petroleum ether latex of *Calotropis Gigantea* within the outer shell layer of vesicle.



[a]  
Figure 3. TEM of (a) CGPHGF and (b) CGHGF

### Rheological studies

In the current study, the hyaluronan acidic chains underwent extensive ionization at  $\text{pH} > 3$  and formed a network of strong intermolecular interaction with viscoelastic features. The viscosity measurements showed that the viscosity of CGHGF is  $735 \pm 4.23$  cp and CGPHGF is shown  $346 \pm 4.17$  cp at the same speed (100 rpm,) confirming the good vesicular gel-core consistency and subsequent higher retention time and prolonged effect. The viscosity of CGHGF  $346 \pm 4.17$  cp was 3-fold higher than that of the CG-Carbopol Gel  $115 \pm 3.53$  cp at the same speed (100 rpm) reflecting the superior gelation efficacy of hyaluronan versus carbopol. Moreover, the results showed that, incorporation of Petroleum ether latex of *Calotropis Gigantea* into hyalurosomes yielded a significant 2-fold reduction in the viscosity of the gel. This result may be ascribed to the effect of positively charged Petroleum ether latex of *Calotropis Gigantea* that induced conformational changes of the hyaluronan chains and led to a decrease in the solution viscosity.

### *In-vitro* release behaviour

The *in-vitro* cumulative release profiles of the Petroleum ether latex of *Calotropis Gigantea* solution, CGHGF and CG-Carbopol Gel in acetate buffer (pH 5) are shown in Figure 4 and stated that release pattern of Petroleum ether latex of *Calotropis Gigantea* solution showed that content was released rapidly and almost completely released after 1h confirming its dialyzability. CG-Carbopol Gel (Conventional gel) showed a biphasic release pattern with an initial burst effect in the first 1h (cumulative drug release of 54% followed by a slower release rate that reached 100% after ~3h. The burst-release of drug could be ascribed to the poor incorporation of latex within the Carbopol matrix leading to rapid partitioning of the hydrophilic into the aqueous release medium. The limited sustained phase may be attributed to the time required for water penetration and polymer erosion that facilitate diffusion of the drug remaining from the Carbopol matrix.

On the other hand, *Petroleum ether latex of Calotropis Gigantea* loaded-hyalurosomes (CGHGF) showed an initial burst-release phase in the first 1h, with a cumulative release rate of ~15%. Then, the release rate slowed, demonstrating typical sustained and prolonged drug-release behaviour that continued for  $\leq 24$ h. This sustained release further confirmed the efficient incorporation of *Petroleum ether latex of Calotropis Gigantea* in the nano-vesicular system. Therefore, more time was required for drug partitioning into the aqueous medium from gel-core hyalurosomes that was considered the predominate step in release. This benefit is expected to provide greater patient compliance because of the need for fewer topical applications.

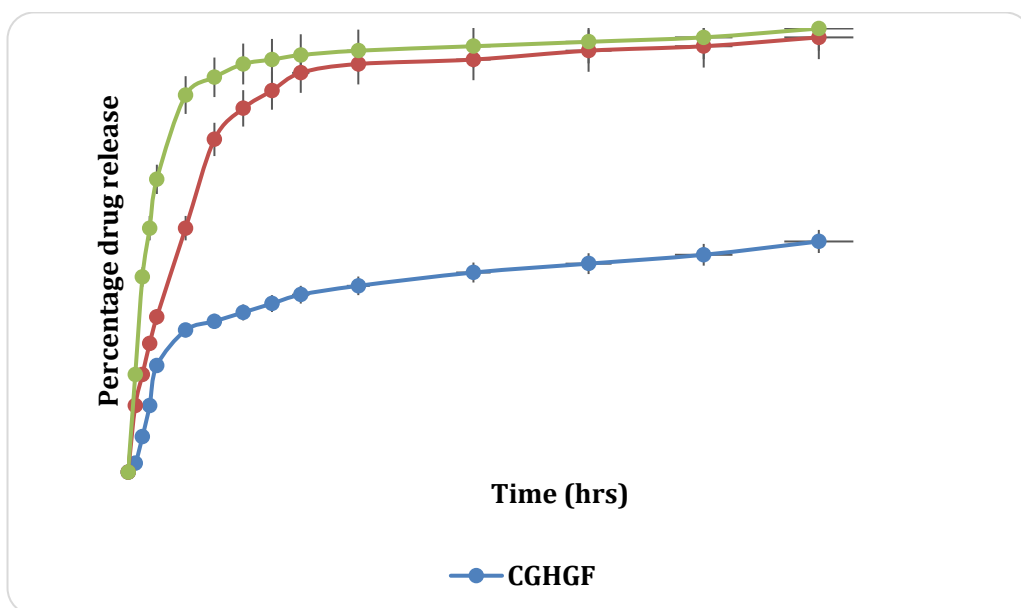


Figure 5. In-vitro cumulative release profile of Petroleum ether latex of *Calotropis Gigantea* solution, CGHGF and CG-Carbopol Gel

## Pharmacological Evaluation

### Evaluation studies on B16F10 cell line

The study constraints in developing animal model for vitiligo, *in vitro* assessment was performed to evaluate the efficacy of CGHGF. Spontaneous and induced animal models developed to evaluate new treatments of vitiligo have their distinct advantages and disadvantages. Induced models may not demonstrate initiating events of vitiligo while spontaneous models which develop in a more physiologic manner can be time-consuming and costly due to low incidence of disease. Hence, mouse melanoma cells (B16F10) which address the experimental questions of present study were chosen to evaluate CGHGF formulations.

### Cell uptake studies

Cell uptake of developed carrier depends on its penetration capacity which is in turn affected by vesicle composition. For this study, cells were exposed to fluorescent Rhodamine-CGHGF and Fluorescent Rhodamine solution at different

concentrations ranging from 1 to 10  $\mu\text{M}$ . Uptake of Fluorescent Rhodamine produced red fluorescence in the cells while nuclear staining by AO produced green fluorescence in the nuclear region. Yellow combinatorial fluorescence was revealed in merged images as a result of combining red fluorescence (Fluorescent rhodamine) and green fluorescence (AO). Increase in uptake of Fluorescent Rhodamine yielded an increase in yellow combinatorial fluorescence. At every tested concentration of Fluorescent Rhodamine, CGHGF carrier showed higher fluorescence intensity compared to solution indicating higher uptake of Fluorescent rhodamine from lipid carrier over solution. This effect might be due to the deformability of CGHGF which enhances its penetration and thereby uptake of loaded moiety.

No significant difference was observed in images of Fluorescent Rhodamine solution from 1 to 10  $\mu\text{M}$  (Figure 6 A-C). For Fluorescent Rhodamine-CGHGF, increase in yellow fluorescence was observed from 1 to 10  $\mu\text{M}$  concentration (Figure 6.1 D-F) reflecting higher uptake of Fluorescent Rhodamine from CGHGF compared to solution. Among Fluorescent Rhodamine-CGHGF, 10  $\mu\text{M}$  CGHGF showed a higher fluorescent intensity (Figure 6.1 F) compared to 1  $\mu\text{M}$  (Figure 6.1D) and 5  $\mu\text{M}$  Fluorescent Rhodamine-CGHGF (Figure 6.1E) which showed a concentration dependent effect. This might be due to higher intracellular accumulation of encapsulated Fluorescent Rhodamine at higher concentration.

Quantitative dye uptake into cells observed for 10  $\mu\text{M}$  dye loaded formulations showed  $60.60 \pm 3.23\%$  uptake with Fluorescent Rhodamine-CGHGF while Fluorescent Rhodamine solution showed about  $32.01 \pm 4.85\%$  uptake of Fluorescent Rhodamine. This showed a 1.89 fold increase in uptake of encapsulated Fluorescent Rhodamine with CGHGF carrier compared to solution. This confirmed the higher uptake of loaded moiety with developed CGHGF carrier which could also assist in improved delivery of CGHGF.

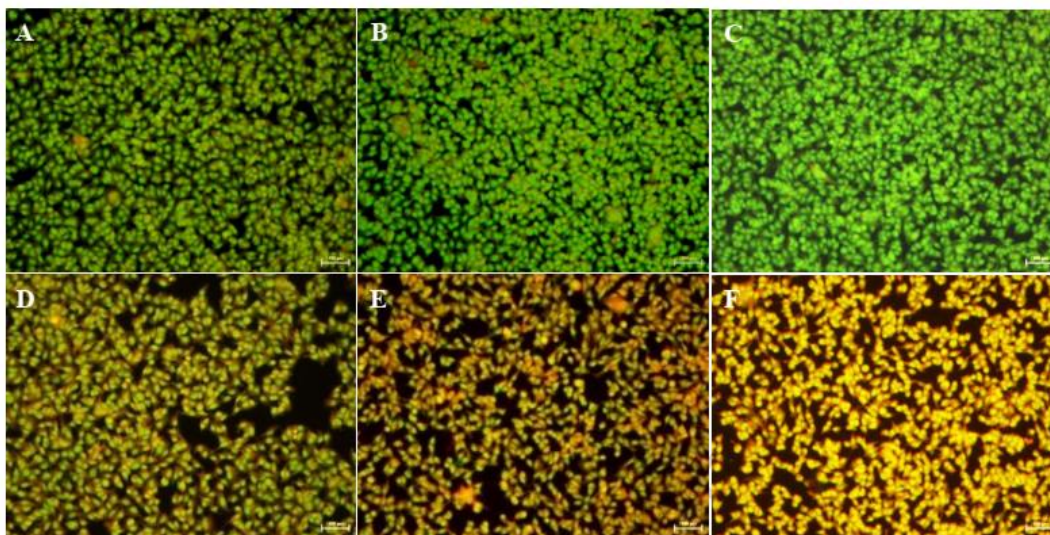


Figure 6. Cell uptake study to determine the penetration capacity of CGHGF

Figure shows merged Fluorescent Rhodamine and AO images of B16F10 cell line exposed to (A) Fluorescent Rhodamine solution (1  $\mu\text{M}$ ), (B) Fluorescent Rhodamine solution (5  $\mu\text{M}$ ), (C) Fluorescent Rhodamine solution (10  $\mu\text{M}$ ), (D) Fluorescent Rhodamine-CGHGF (1  $\mu\text{M}$ ), (E) Fluorescent Rhodamine-CGHGF (5  $\mu\text{M}$ ) and (F) Fluorescent Rhodamine- CGHGF (10  $\mu\text{M}$ ) for 3 h (bar represents 1000  $\mu\text{m}$ ). Uptake of Fluorescent Rhodamine produced red fluorescence in cells while AO staining produced green fluorescence in the nuclear region. Merge of red and green fluorescence revealed yellow combinatorial fluorescence. Higher fluorescence intensity was observed with Fluorescent Rhodamine-CGHGF compared to Fluorescent Rhodamine-Solution at every concentration indicating higher uptake of Fluorescent Rhodamine from lipid carrier over solution.

Membrane fluidity of CGHGF due to 1- $\alpha$ -phosphatidylcholine and vesicle deformability due to presence of Sodium deoxy cholate (SDC) enhanced the uptake of dye loaded CGHGF compared to solution. This is in agreement with previous reports where synergistic effect of 1- $\alpha$ -phosphatidylcholine combination on fluidity of bilayer membrane and structural deformability due to SDC improved penetration of lipid nanocarriers. These observations proved that the optimized vesicle composition was successful in obtaining the penetration of encapsulated moieties.

### **Cell viability assay**

This study was performed to decide on the concentration that exhibits maximum stimulatory effect on pigmentation parameters with minimal cytotoxic effect. Initially, this assay was done using Petroleum latex of *Calotropis Gigantea* as drug (0.25%w/w, 5 mg) to determine  $\text{IC}_{50}$ , the concentration which inhibits 50% cell viability and in-turn ascertain working concentration range. From this assay, CGHGF showed 68.71 $\pm$ 2.76% cytotoxicity, Petroleum latex of *Calotropis Gigantea* solution showed 22.10 $\pm$ 9.63% cytotoxicity and CG-Carbopol Gel showed 52.10 $\pm$ 9.63% cytotoxicity at 50 $\mu\text{M}$  concentration (Figure 7A). Further, MTT assay was performed to evaluate the cytotoxic effect of different test formulations i.e., Latex solution, test formulations (CG-Carbopol Gel) and Petroleum latex of *Calotropis Gigantea* loaded-hyalurosomes (CGHGF) on B16F10 cells. All the formulations were tested at respective drug concentration ranging from 1 to 50  $\mu\text{M}$  (this concentration range was selected based on the results of initial cell viability assay). Dose dependent increase in cytotoxicity was observed with all the formulations and the cytotoxicity observed with drug loaded CGHGF was slightly higher compared to respective drug solution (Figure 7B). A concentration which shows therapeutic efficacy with minimal toxicity has to be selected for further studies.

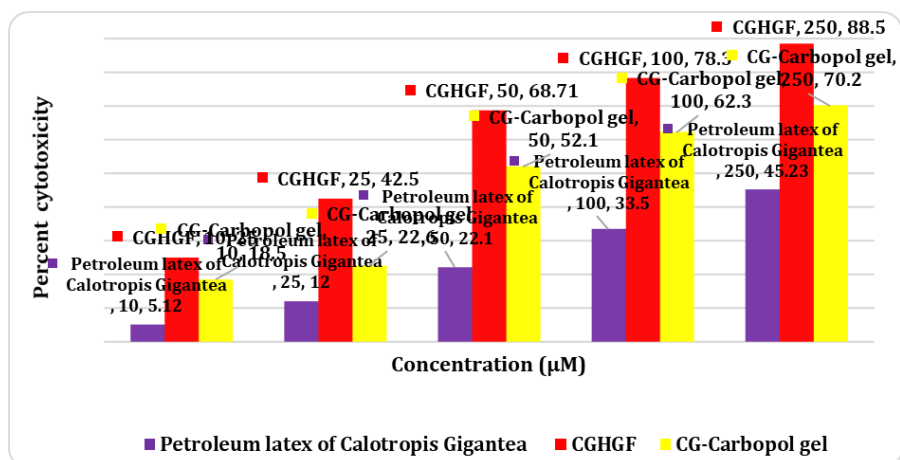


Figure 7 (A). Cell Viability study of Petroleum latex of *Calotropis Gigantea*, CGHGF and CG-Carbopol gel

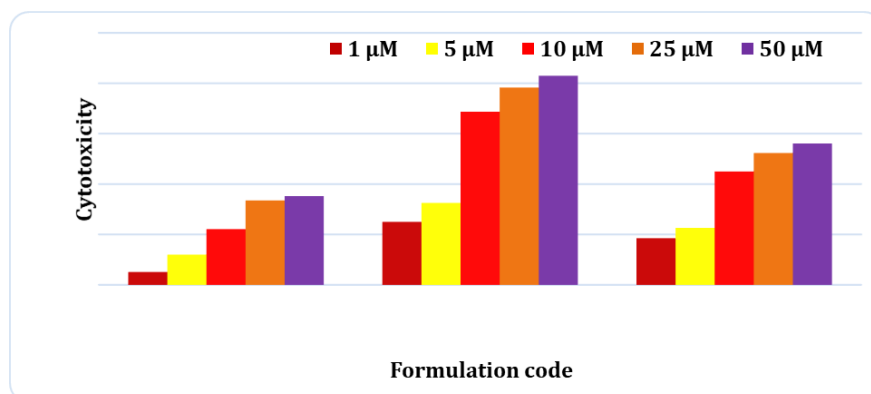


Figure 7 (B). Effect of different nano-formulation on cell viability, B16F10 cells were exposed to different formulation i.e., Petroleum latex of *Calotropis Gigantea*, CGHGF and CG-Carbopol gel in concentration range 1-50 µM. All data represent mean±SD (n=3)

The Latex solution has shown the CG-Carbopol gel showed 56.11±11.55% cytotoxicity at 50 µM concentration of Latex while showed CGHGF 82.95±11.61% cytotoxicity at 50 µM concentration of latex. Low drug concentrations i.e., 1 µM and 5 µM showed minimal cytotoxicity with all the formulations. Latex solution showed about 12.24±7.37% and CGHGF showed 32.5.10±0.46% cytotoxicity at 5 µM concentration. CG-Carbopol gel showed 22.6±1.56% cytotoxicity at 5 µM concentration (Figure 6B). As above 60% of cells are viable in all the formulations at 5 µM equivalent drug concentration, this was selected as working concentration for further studies. The *Petroleum latex of Calotropis Gigantea* showed dose dependent therapeutic effect by stimulation of melanogenesis and tyrosinase activity at a concentration ranging from 1 to 10 µM.

### Melanin and tyrosinase activity assay

Petroleum latex of *Calotropis Gigantea* may acts in vitiligo by stimulating melanization, increased synthesis of tyrosinase via cAMP activity and by photo-polymerization of melanogenic precursors. In this study, the effect of Latex solution, test formulations (CG-Carbopol Gel) and Petroleum latex of *Calotropis Gigantea* loaded hyalurosomes (CGHGF) on melanin content and tyrosinase activity was determined. These parameters were evaluated in terms of first treatment (cells were treated once) and second treatment (cells were treated twice).

Melanin is a natural pigment that plays a vital role in skin pigmentation and destruction of melanocytes leads to depigmentation which is the pathological hallmark of vitiligo. Compared to control (85 relative melanin content), Petroleum latex of *Calotropis Gigantea* solution showed an increase in melanin content by 1.20 fold upon first treatment ( $p < 0.05$ ) and 1.20 fold upon second treatment ( $p < 0.05$ ). CGHGF is showed a 2.25 fold increase in melanin with first treatment ( $p < 0.0001$ ) and a 2.89 fold increase with second treatment ( $p < 0.0001$ ). This showed that effect of PUVA with CGHGF showed enhanced stimulation of melanin levels compared to Petroleum latex of *Calotropis Gigantea*. CGHGF showed a significant difference in melanin proportion between first and second treatment levels ( $p < 0.05$ ) which indicates dose dependent elevation of melanin content.

For Petroleum latex of *Calotropis Gigantea* solution and CG-Carbopol Gel, significant increase in melanin content was observed in comparison with control. This confirmed that has either inhibitory or stimulatory effects on melanin content at 5  $\mu\text{M}$  working concentration. For CG-Carbopol Gel, there was 2.05 fold increase in melanin content with first treatment ( $p < 0.01$ ) while 2.64 fold increase was observed with second treatment ( $p < 0.01$ ) (Figure 8A).

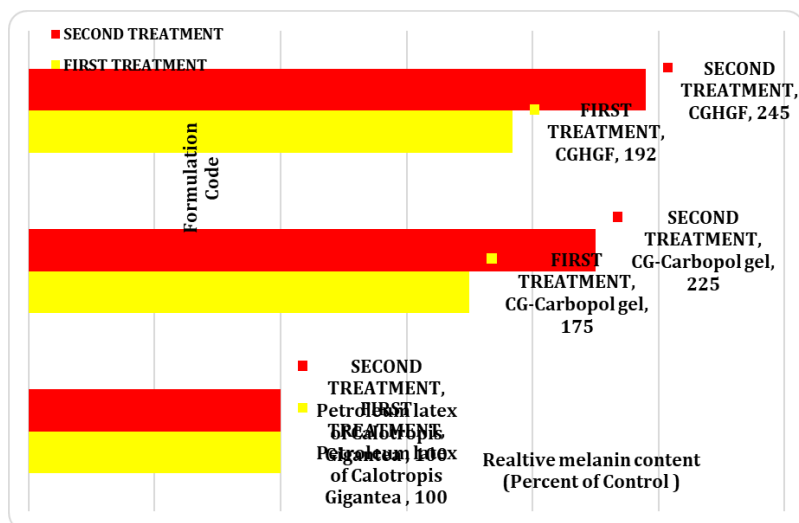


Figure 8 (A). Effect of different Nano-formulation on relative melanin content in B16F10 cells

Tyrosinase is considered as the key determinant of pigmentation and as rate limiting enzyme for melanin synthesis. CGHGF showed a significant increase in tyrosinase activity by 2.64 fold with first treatment ( $p < 0.001$ ) and 2.72 fold increase with second treatment ( $p < 0.0001$ ) compared to control while a very slight increase in tyrosinase activity was observed with Petroleum latex of *Calotropis Gigantea* solution. (Figure 8B) This ensured enhanced therapeutic effect of PUVA with CGHGF compared to Petroleum latex of *Calotropis Gigantea* solution.

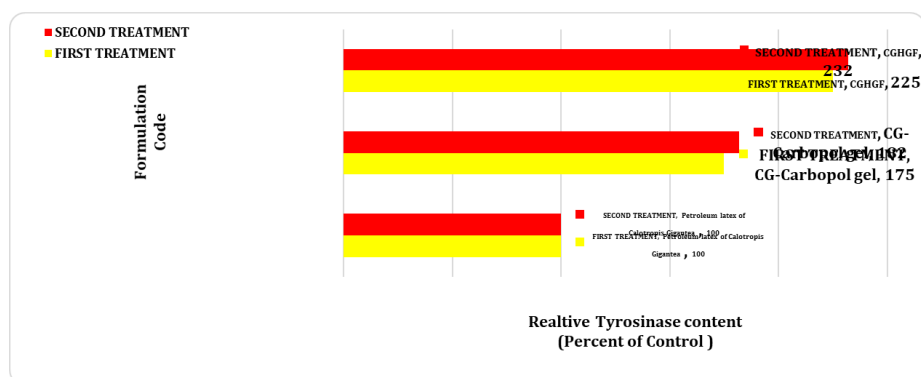


Figure 8 (B). Effect of different Nano-formulation on relative tyrosinase activity in B16F10 cells

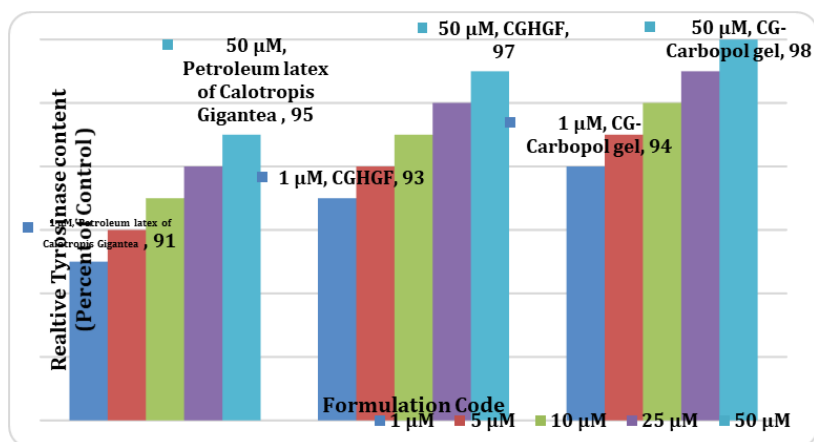


Figure 8 (C). Cell free tyrosinase assay to determine the direct effect of different formulation on tyrosinase activity

In a cell free system, tyrosinase assay was performed with mushroom tyrosinase and LDOPA to determine the direct effect of Petroleum latex of *Calotropis Gigantea* formulations on tyrosinase activity. No significant difference was observed in tyrosinase activity with any of the formulation groups compared to control (Figure 8C). This showed that Petroleum latex of *Calotropis Gigantea* did not have direct effects on tyrosinase activity. This is in support with a previous report which stated indirect effect of PSR on tyrosinase synthesis via cAMP that further increases tyrosinase enzymatic activity.

### Fontana-Masson silver staining

This staining is performed to visualize melanin pigment in cells exposed to *Petroleum latex of Calotropis Gigantea* CGHGF formulations.

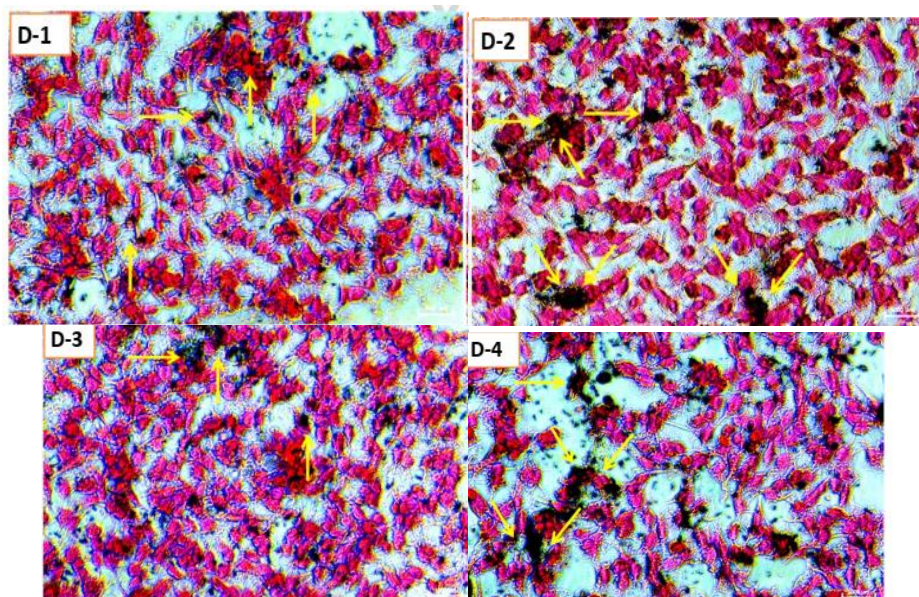


Figure 8D. Fontana-Masson silver staining to visualize melanin pigment in B16F10 cell line where melanin is stained by dark black (indicated by arrows). D-1= Control, D-2= Petroleum latex of *Calotropis Gigantea* solution, D-3= CG-Carbopol Gel and D-4= CGHGF

It is a histochemical technique based on oxidation of melanin and reduction of silver resulting in a black stain that can be visualized under microscope. Compared to the control (Figure 8D-1), the amount of melanin granules was significantly increased and stained in Petroleum latex of *Calotropis Gigantea* solution (Figure 8D-2), CG-Carbopol Gel (Figure 8D-3) and CGHGF (Figure 8D-4) groups (indicated by yellow arrows in figure). The obtained results were in agreement with the results obtained with melanin content and tyrosinase assay.

### Conclusion

The currently marketed treatments for vitiligo have shown limited effectiveness, which has created a substantial demand for novel vitiligo treatments. The CGPHGF (Placebo-hyalurosomes), *Petroleum latex of Calotropis Gigantea* loaded-hyalurosomes (CGHGF) and CG-Carbopol Gel were successfully prepared with particle size of <150 nm and high entrapment efficiency. Unique deformable nature of hyalurosomes and CG-Carbopol gel also assists in skin penetration enhancement of latex containing active constituents. Higher encapsulation of loaded drugs reduces the drug dose and sustained release of *Petroleum latex of Calotropis Gigantea* loaded-hyalurosomes (CGHGF) and CG-Carbopol Gel avoids frequent drug administration. Cell uptake studies confirmed higher penetration of encapsulated moiety through prepared CGHGF.

The topical *Petroleum latex of Calotropis Gigantea* loaded-hyalurosomes (CGHGF) investigated in this study showed outstanding properties for effective treatment of vitiligo through permitting its delivery into human skin with a high deposition level. Moreover, this delivery system utilized a new platform for the localized topical treatment of vitiligo to minimize the side effects of systemic therapies, which could represent a pivotal improvement in treatment. In conclusion, *Petroleum latex of Calotropis Gigantea* loaded-hyalurosomes (CGHGF) hyalurosomes investigated in this study showed promising skin permeation and deposition properties that should be highly useful for clinical treatment of numerous skin-disorder.

**Conflict of Interest:** Nil.

## References

1. Ahmad W. Preliminary phytochemical, antimicrobial and photochemical study of *Calotropis Gigantea* leaf extract. *Cur Chem Lett* 2020; 9: 105-112.
2. Alafnan A, Sridharagatta S, Saleem H, Khurshid U, Alamri A, Ansari SY, Zainal Abidin SA, Ansari SA, Alamri AS, Ahemad N and Anwar S. Evaluation of the Phytochemical, Antioxidant, Enzyme Inhibition, and Wound Healing Potential of *Calotropis Gigantea* (L.) Dryand: A Source of a Bioactive Medicinal Product. *Front Pharmacol* 2021; 12: 70136
3. Alam MA, Habib MR, Fajarna N, Khalequzzarnafr M, Karim MR. Insectisidal activity of root bark of *Calotropis Gigantea* L. against *Triboliun Castaneum* (Herbst). *World Journal of Zoology* 2009; 4(2): 90-95.
4. Alluri N, Majumdar M. Phytochemical analysis and in vitro antimicrobial activity of *Calotropis Gigantea*, *Lawsonia inermis* and *Trigonella foecum Graecum*. *Int J Pharm Pharm Sci* 2014; 6(4): 524-527.
5. Bharathi P, Thomas A, Thomas S, Krishnan S, Ravi TK. Anti-bacterial activity of leaf extracts of *Calotropis Gigantea* linn. against certain Gram-negative and Gram-positive bacteria. *Int J Chem Sci* 2011; 9: 919-23.
6. Chandrabhan S, Sumint ST. Antibacterial efficacy and phytochemical analysis of organic solvent extracts of *Calotropis Gigantea*. *J Chem Pharm Res* 2011; 3(6): 330-336
7. David M, Bharath KR, Bhavani M. Study of *Calotropis Gigantea* R. Br. extracts on growth and survival dynamics of selected pathogenic microorganisms. *Int J Bio Engg* 2011; 1(1): 1-5.
8. Elhalmoushy PM, Elsheikh MA, Matar NA, El-Hadidy WF, Kamel MA, Omran GA, Elnaggar YSR. Novel berberine-loaded hyalurosomes as a promising nanodermatological treatment for vitiligo: Biochemical, biological and gene expression studies. *International Journal of Pharmaceutics* 2022; 615: 121-130.
9. Habib MR, Karim MR. Effect of anhydrosophoradiol-3-acetate of *Calotropis Gigantea* (Linn.) flower as antitumor agent against Ehrlich's ascites carcinoma in mice. *Pharmacol Rep* 2013; 65: 761-767
10. Hasballah K. Antibacterial activity of methanol extract of *Calotropis Gigantea* Flowers from Aceh. 2018; 3(4): 196-200.
11. Hemalatha M, Arirudran B. Antimicrobial effect of separate extract of acetone, ethyl acetate, methanol and aqueous from leaf of milkweed (*Calotropis gigantea* L. *Asian J Pharm Res* 2011; 1(4): 102-107.

12. Hoopes GM, Hamilton JP, Kim J, Zhao D, Wiegert-Rininger K, Crisovan E, Buell CR. Genome assembly and annotation of the medicinal plant *Calotropis gigantea*, a producer of anticancer and antimalarial Cardenolides. *G3 Bethesda* 2018; 8(2): 385–91.
13. Jain NS, Pushpendra NK, Navneet K, Pathak G, Mehta SC. *In-vitro* antioxidant activity of *Calotropis Gigantea* hydroalcoholic leaves extract. *Der Pharma Lett* 2010; 2(3): 95-100.
14. Jain V, Nath B, Gupta GK, Shah PP, Siddiqui MA, Pant AB, Mishra PR. Galactose grafted chylomicron-mimicking emulsion: evaluation of specificity against HepG-2 and MCF-7 cell lines. *J Pharm Pharmacol* 2009;61(3): 303–310
15. Jiyon L, Jang H-J, Chun H, Pham T-H, Bak Y, Shin J-W, Jin H, Kim Y-I, Ryu HW, Ryang Oh, Yoon D-Y. *Calotropis gigantea* extract induces apoptosis through extrinsic/intrinsic pathways and reactive oxygen species generation in A549 and NCI-H1299 non-small cell lung cancer cells. *BMC Comp Alter Med* 2019; 19: 134
16. Kumar G, Karthik L, Bhaskara Rao KV. Antibacterial activity of aqueous extract of *Calotropis gigantea* leaves - an in-vitro study. *Int J Pharm Sci Rev Res* 2010; 4(2): 141-144
17. Kumar G, Karthik L, Rao KV. Antimicrobial activity of latex of *Calotropis Gigantea* against pathogenic microorganisms—An *in vitro* study. *Pharmacol Online* 2010; 3: 155–63.
18. Kumar G, Loganathan K, Kokati VBR. A Review on Pharmacological and Phytochemical profile of *Calotropis Gigantea* Linn. *Pharmacology online*. 2011; 1: 1-8.
19. Kumar PS, Suresh E and Kalavathy S; Review on a potential herb *Calotropis Gigantea (L.) R. Br.* *Scholars Acad J Pharm* 2013, 2; 2:135–143
20. Lima RC, Silva MCC, Aguiar CCT. Anticonvulsant action of *Calotropis procera* latex proteins. *Epilepsy & Behavior* 2012; 23(2): 123–126.
21. Mandepudi D, Ravuru BK, Mandepudi B. Efficacy of *Calotropis gigantea* R. Br. Extracts as antimicrobial agents on selected pathogenic microorganisms. *Res Bioscientia* 2010; 1(1): 13-18
22. Mir-Palomo S, N'acher A, Buso MOV, Caddeo C, Manca ML, Manconi M, DíezSales O. Baicalin and berberine ultradeformable vesicles as potential adjuvant in vitiligo therapy. *Colloids and Surfaces B: Biointerfaces* 2019; 175: 654–662.
23. Mutiah R, Widyawaruyanti A, Sukardiman S. Calotroposid a: a glycosides Terpenoids from *Calotropis gigantea* induces apoptosis of Colon Cancer WiDr cells through cell cycle arrest G2/M and caspase 8 expression. *Asian Pac J Cancer Prev*. 2018; 19(6): 1457–64
24. Nenaah G. Antimicrobial activity of *Calotropis Procera* Ait. (Asclepiadaceae) and isolation of four flavonoid glycosides as the active constituents. *World J Micro Biotech* 2013; 29(7): 1255–1262.
25. Obese E, Ameyaw E, Biney R, Henneh I, Edzeamey F, Woode E. Phytochemical screening and anti-inflammatory properties of the hydroethanolic leaf extract of *Calotropis Procera* (ait). *R. Br. (Apocynaceae) J Pharm Res Int* 2018; 23(1): 1–11.
26. Obese E, Ameyaw EO, Biney RP, Adakudugu EA, Woode E. Neuropharmacological Assessment of the Hydroethanolic Leaf extract of

- Calotropis Procera* (Ait). R. Br. (Apocynaceae) in Mice. *Scientifica* 2021; 3(4): 10.
27. Obese E, Biney RP, Henneh IT. Antinociceptive effect of the hydroethanolic leaf extract of *Calotropis Procera* (Ait) R. Br. (Apocynaceae): possible involvement of glutamatergic, cytokines, opioidergic and adenosinergic pathways," *Journal of Ethnopharmacology*. 2021; 278; 114-120.
  28. Periyakaruppan PK, Dharman G, Murugaraj J, Murugan AM, Mariappan R. Assembling of multifunctional latex-based hybrid nanocarriers from *Calotropis gigantea* for sustained (doxorubicin) DOX releases. *Biomedicine & Pharmacotherapy* 2017; 87: 461–470.
  29. Rajamohan S, Kalaivanan P, Sivangnanam H, Rajamanickam M. Antioxidant, Antimicrobial activities and GC-MS analysis of *Calotropis gigantea* white flowers. *J Phytopharmacol* 2014; 3(6): 405-409.
  30. Sachin S, Rani A, Nagarathna A, Murugan R, Balasubramanian S. Phytochemical studies on the methanolic extract of *Calotropis Gigantea* leaves Indo Am J P Sci 2018; 5(7); 6248-6260.
  31. Sanyal S, Maity P, Pradhan A. Sub-acute toxicity study of *Calotropis gigantea* latex extracts in male Swiss albino mice. *Toxicol Forensic Med Open J* 2016; 1(2): 54-64.
  32. Saratha V, Subramanian SP. Evaluation of antifungal activity of *Calotropis gigantea* latex extract: an in vitro study. *Int J Pharma Sci Res* 2010; 1(9): 88-96.
  33. Seeka C, Sutthivaiyakit S. Cytotoxic cardenolides from the leaves of *Calotropis Gigantea*. *Chem Pharm Bull (Tokyo)* 2010; 58(5): 725-728.
  34. Seniya C, Trivedia SS, Verma SK. Antibacterial efficacy and phytochemical analysis of organic solvent extracts of *Calotropis gigantea*. *J Chem Pharm Res* 2011; 3(6): 330-336.
  35. Sharma M, Tandon S, Nayak UA, Kappadi D, Rathore AS, Goyal A. *Calotropis gigantea* as a potential anticariogenic extract agents against *Streptococcus mutans*: An *in-vivo* comparative evaluation. *J Conserv Dent* 2017; 20(3): 174–179.
  36. Sharma N, Shankar R, Gupta N, Prakash P. A preliminary phyto pharmacognostical evaluation of *Calotropis gigantea* (L.) R. Br. (Alarka or Mandara) Root. *Int J Ayur Med* 2016; 7(1):44–48.
  37. Singh M, Javed K; Comparative study of chemical composition of *Calotropis Gigantea* flower, leaf and fruit essential oil. *Eur Chem Bull* 2015; 4(10):577–480.
  38. Srivastava S, Singh A, Rawat A. Comparative Botanical and Phytochemical Evaluation of *Calotropis Procera* Linn and *Calotropis Gigantea* Linn. Root. *J App Pharm Sci* 2015; 5: 41-47
  39. Sun MC, Xu XL, Lou XF, Du YZ. Recent Progress and Future Directions: The Nano-Drug Delivery System for the Treatment of Vitiligo. *Int J Nanomed* 2021; 15: 32-47.